

The transformation of Lepidocrocite (γ -FeOOH) with Fe(II)_(aq) in slightly acidic media: Intermediate pathways and biomimetic behavior

Mario Alberto Gomez^{1,2§}, Yiwen Chen², Miao Song^{3§}, Dongsheng Li³, Alan Scott Lea⁴, Shuhua Yao², Yihang Duan⁵, Yongfeng Jia⁵, Yige Cai¹, and Tangfu Xiao¹

¹*School of Environmental Science and Engineering, Guangzhou University, Guangzhou, Guangdong, China, 510006*

²*Liaoning Engineering Research Center for Treatment and Recycling of Industrially Discharged Heavy Metals, Shenyang University of Chemical Technology, Shenyang, Liaoning, China, 110142*

³*Physical and Computational Science Directorate, Pacific Northwest National Laboratory, Richland, Washington, USA, 99352*

⁴*Environmental and Biological Sciences Directorate, Pacific Northwest National Laboratory, Richland, Washington, USA, 99352*

⁵*Key Laboratory of Pollution Ecology and Environmental Engineering, Institute of Applied Ecology, Chinese Academy of Sciences, Shenyang, Liaoning, China, 110016*

§ Both authors contributed equally to this work

*Corresponding authors: Telephone: +86 13502444282; Fax: +86 15093716277

Telephone: 1 5093716277; Fax: 1 5093716242

E-mail addresses: mario.gomez@gzhu.edu.cn (M. A. Gomez) and Dongsheng.Li2@pnnl.gov (D. Li)

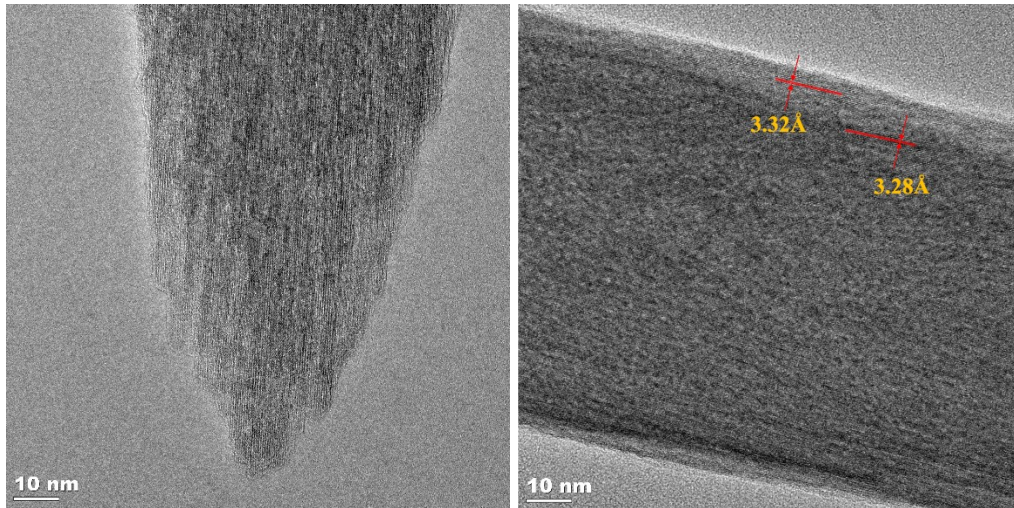


Figure S1. TEM image of the initial LP particles before reaction. Lattice fringe spacing at 3.28Å for the (021) plane was observed.

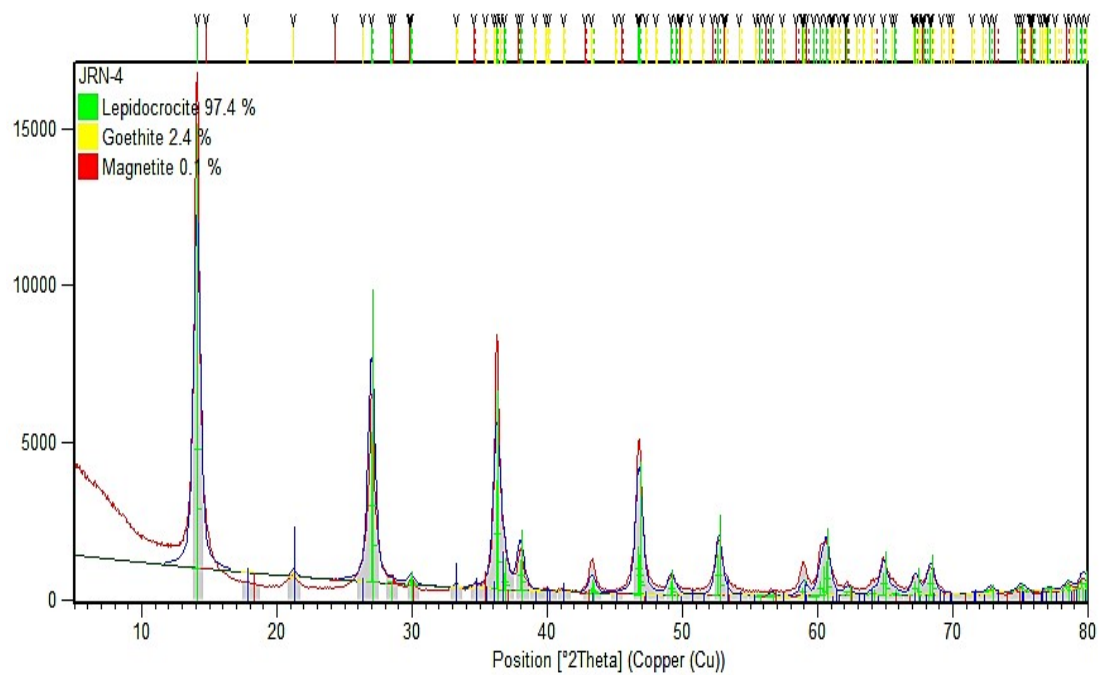


Figure S2. XRD of the initial LP particles before reaction and quantification via Rietveld analysis using the X'Pert Highscore Plus Software.

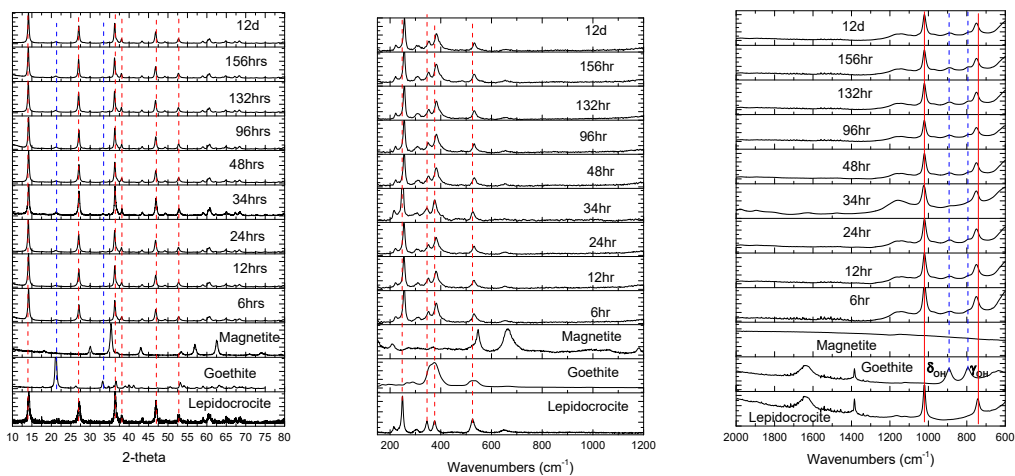


Figure S3. Bulk (a) XRD, (b) Raman, and (c) ATR-FTIR of LP particles reacted with 10 mM Fe(II)_(aq) at various times.

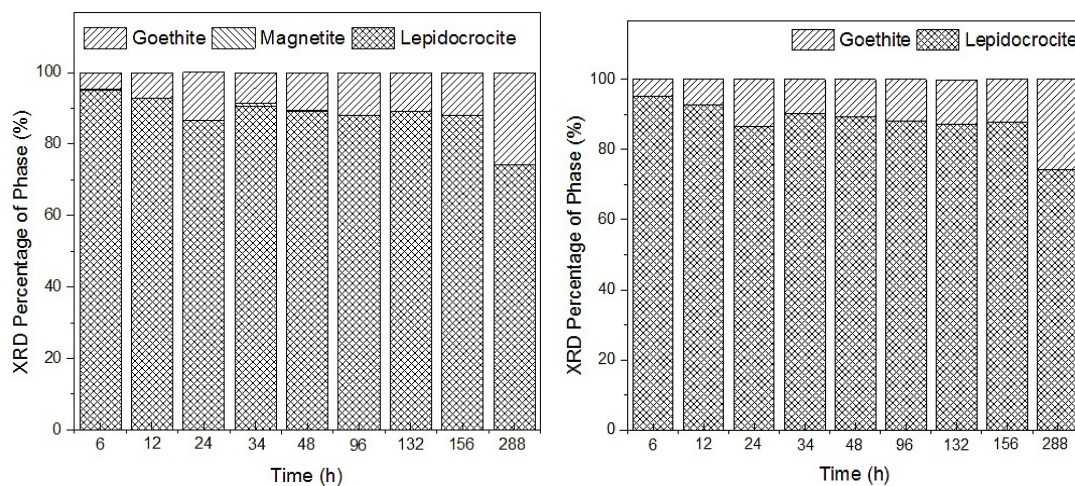


Figure S4. XRD Phase quantification Rietveld analysis using X'pert HighScore of LP particles reacted with 10 mM Fe(II)_(aq) at various times.

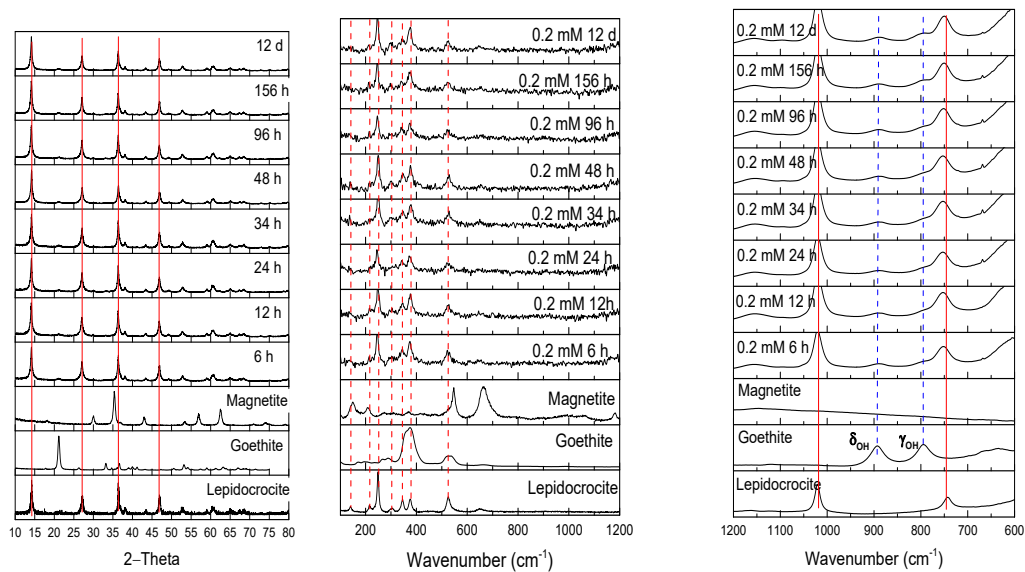


Figure S5. Bulk (a) XRD, (b) Raman, and (c) ATR-FTIR of LP particles reacted with 0.2 mM Fe(II)_(aq) at various times.

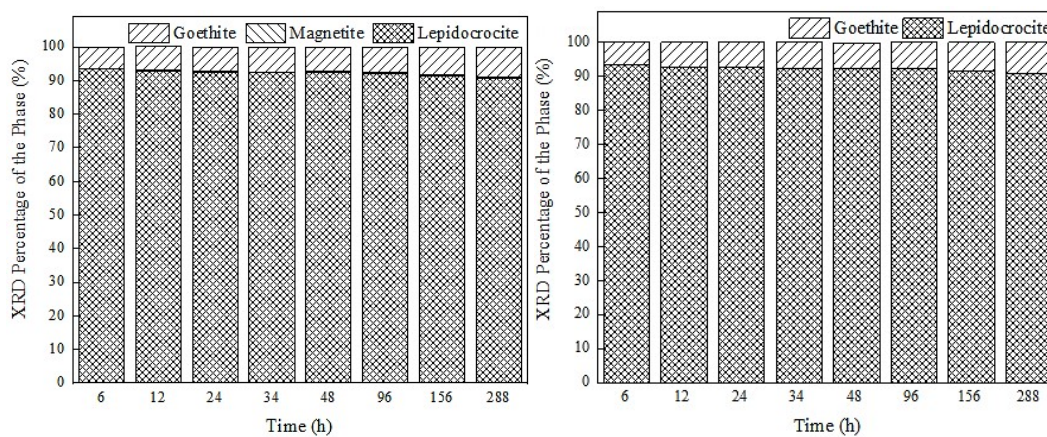
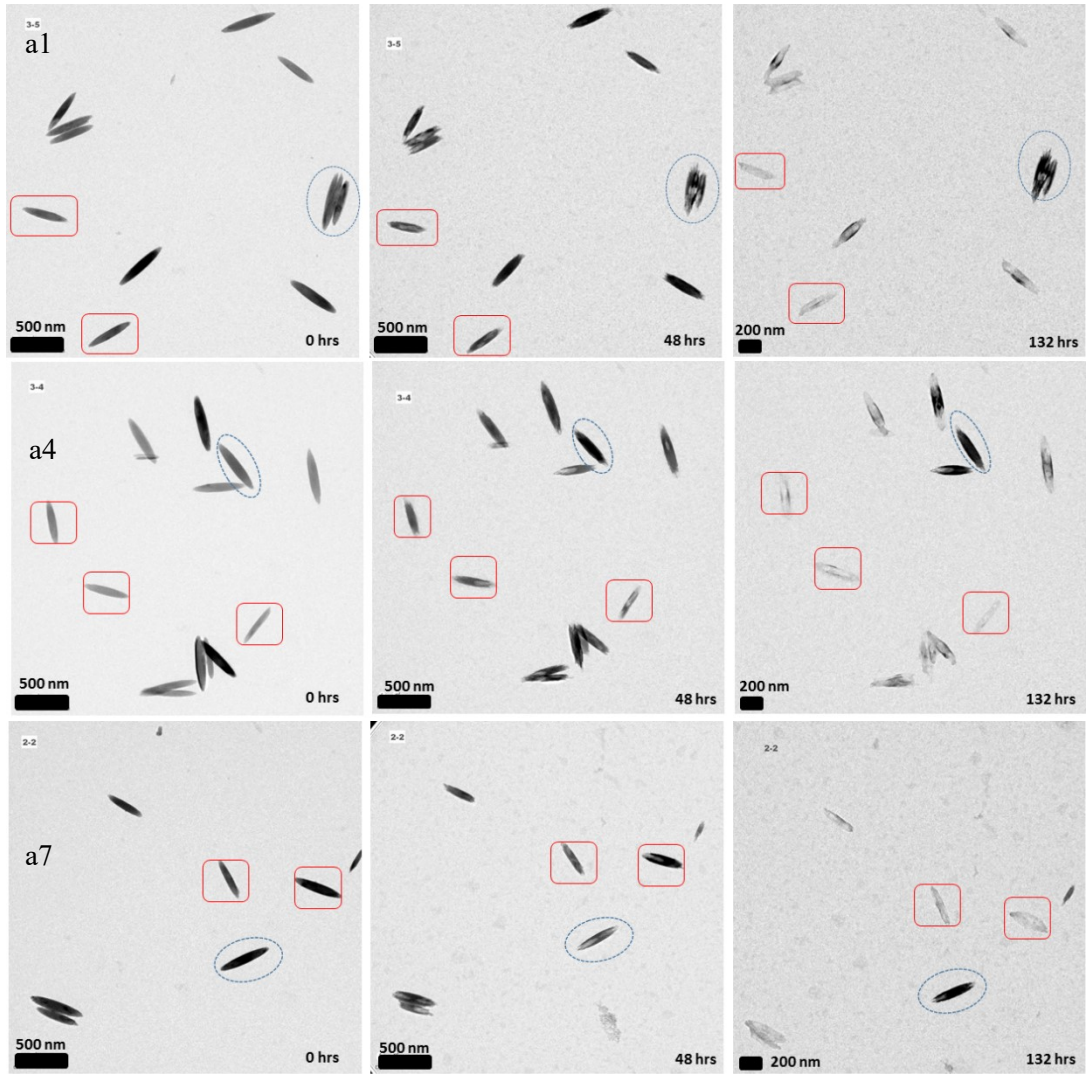


Figure S6. XRD Phase quantification Rietveld analysis using X'pert HighScore of LP particles reacted with 0.2 mM Fe(II)_(aq) at various times.



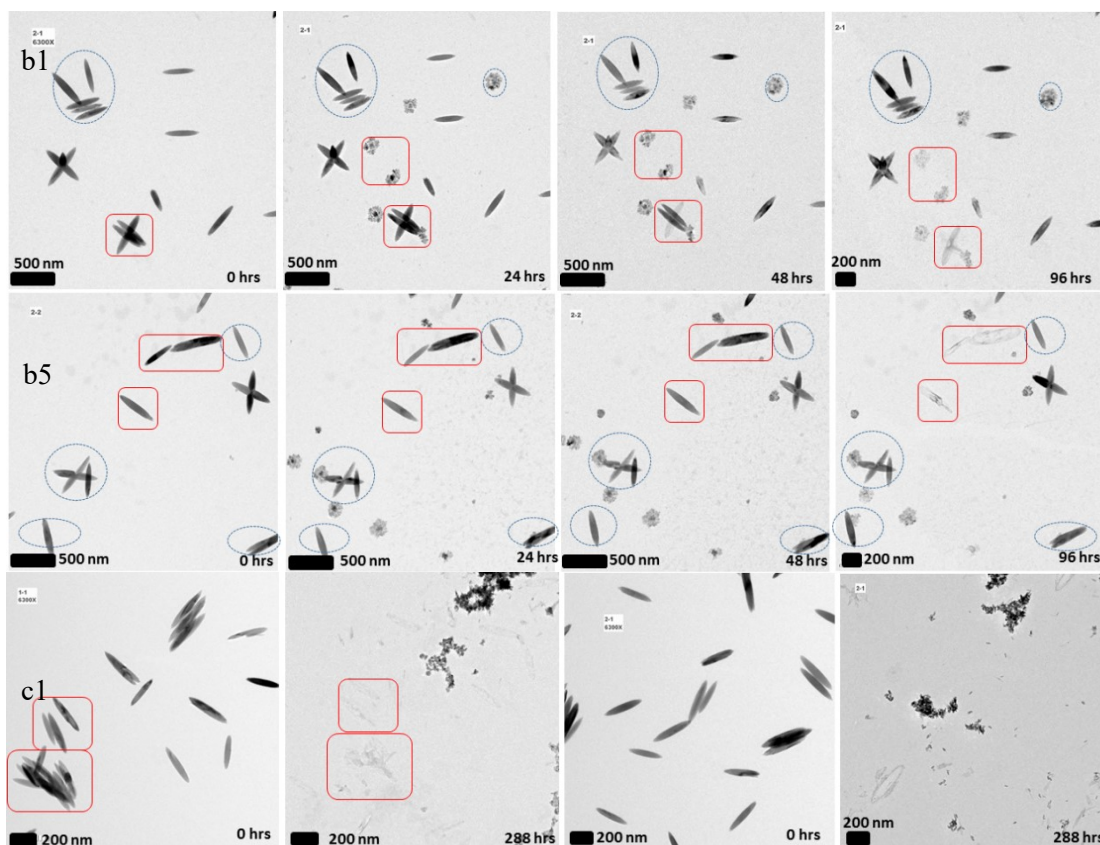


Figure S7. TEM of LP particles upon reaction with 10mM Fe(II)_(aq) after 24hrs, 48hrs, 96hrs, 132hrs, and 288hrs. The selected particles with solid boxes around them show complete dissolution, and the dashed circled particles show the lack of dissolution occurring at various reaction times.

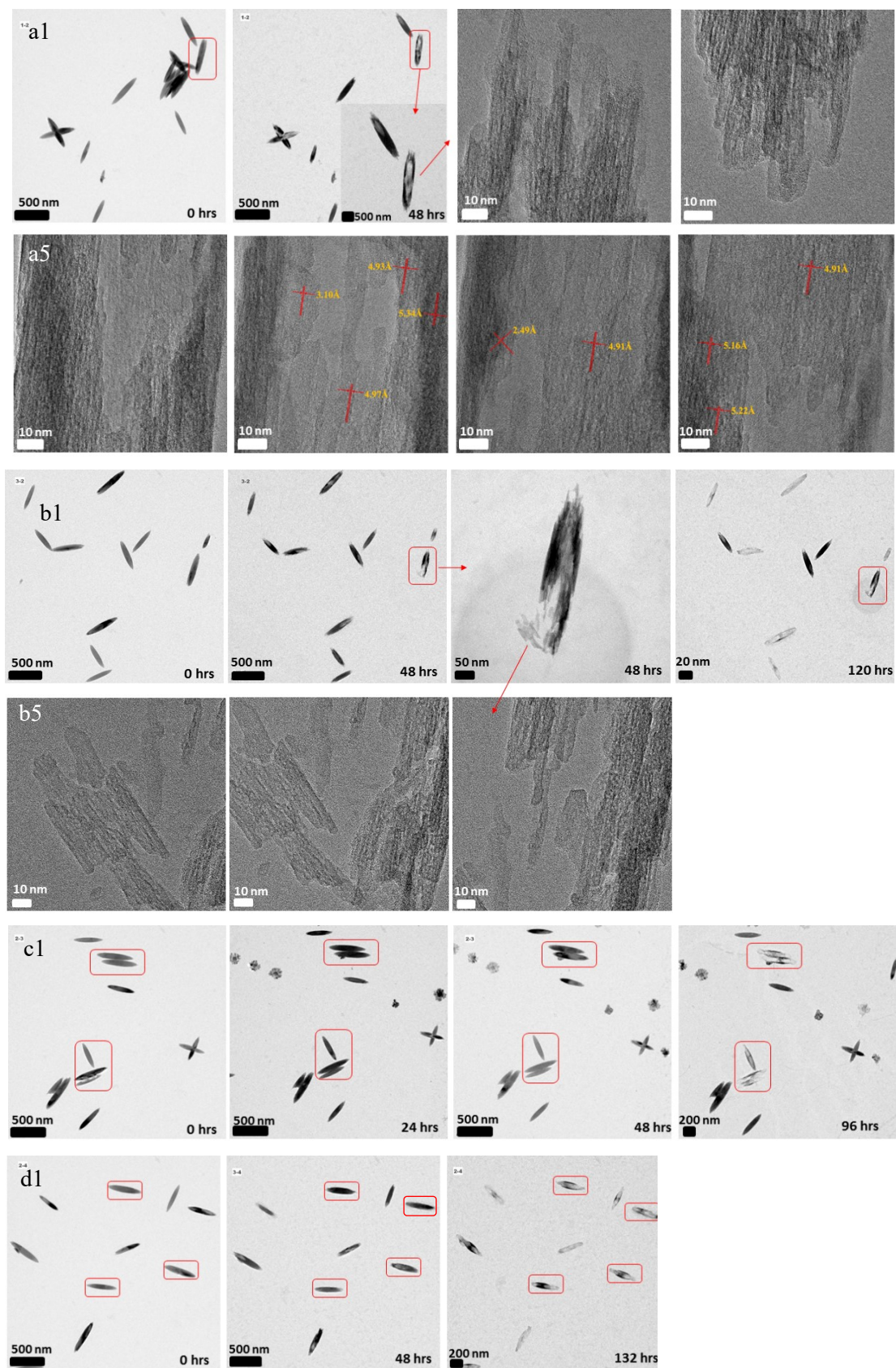
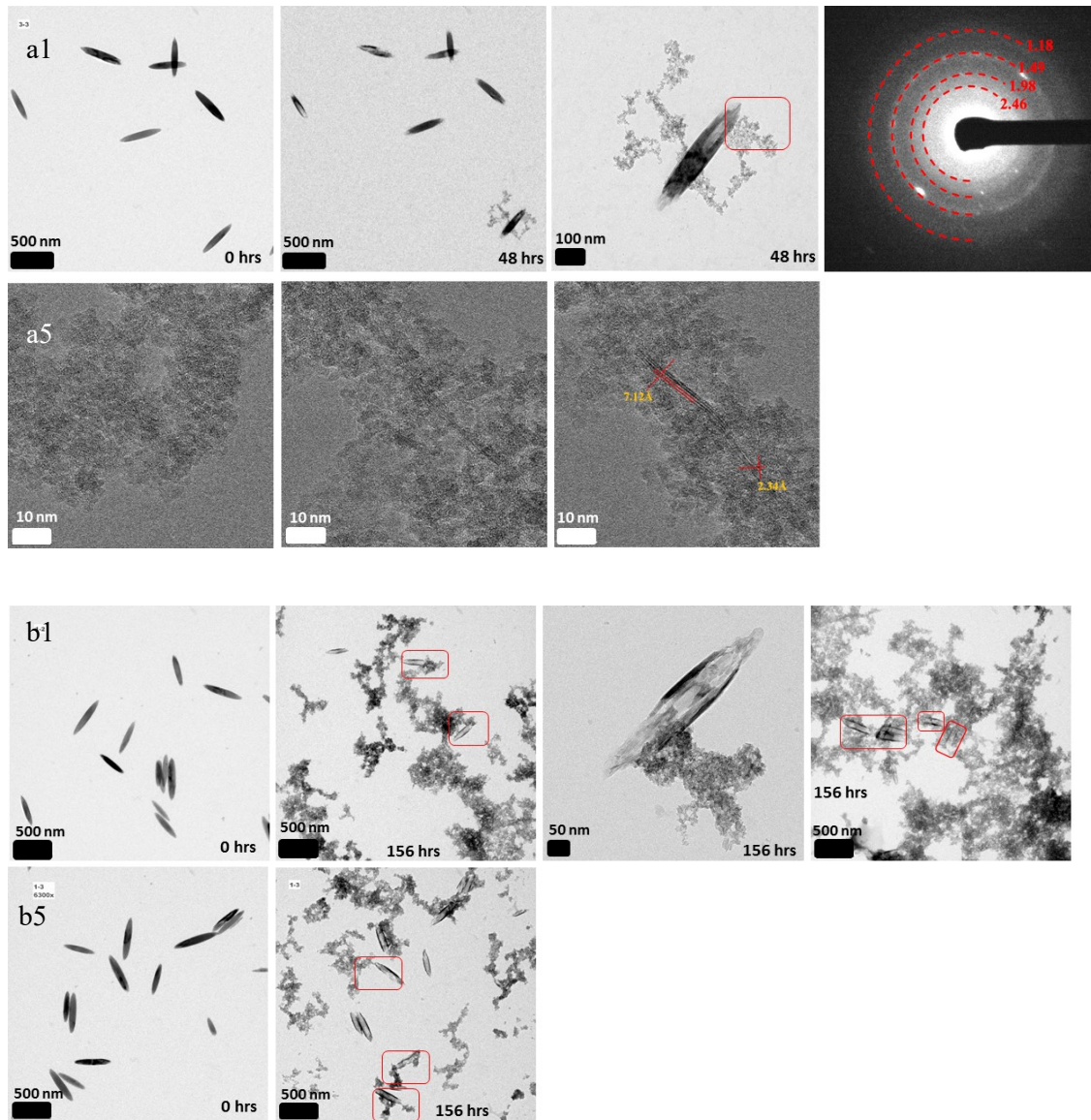
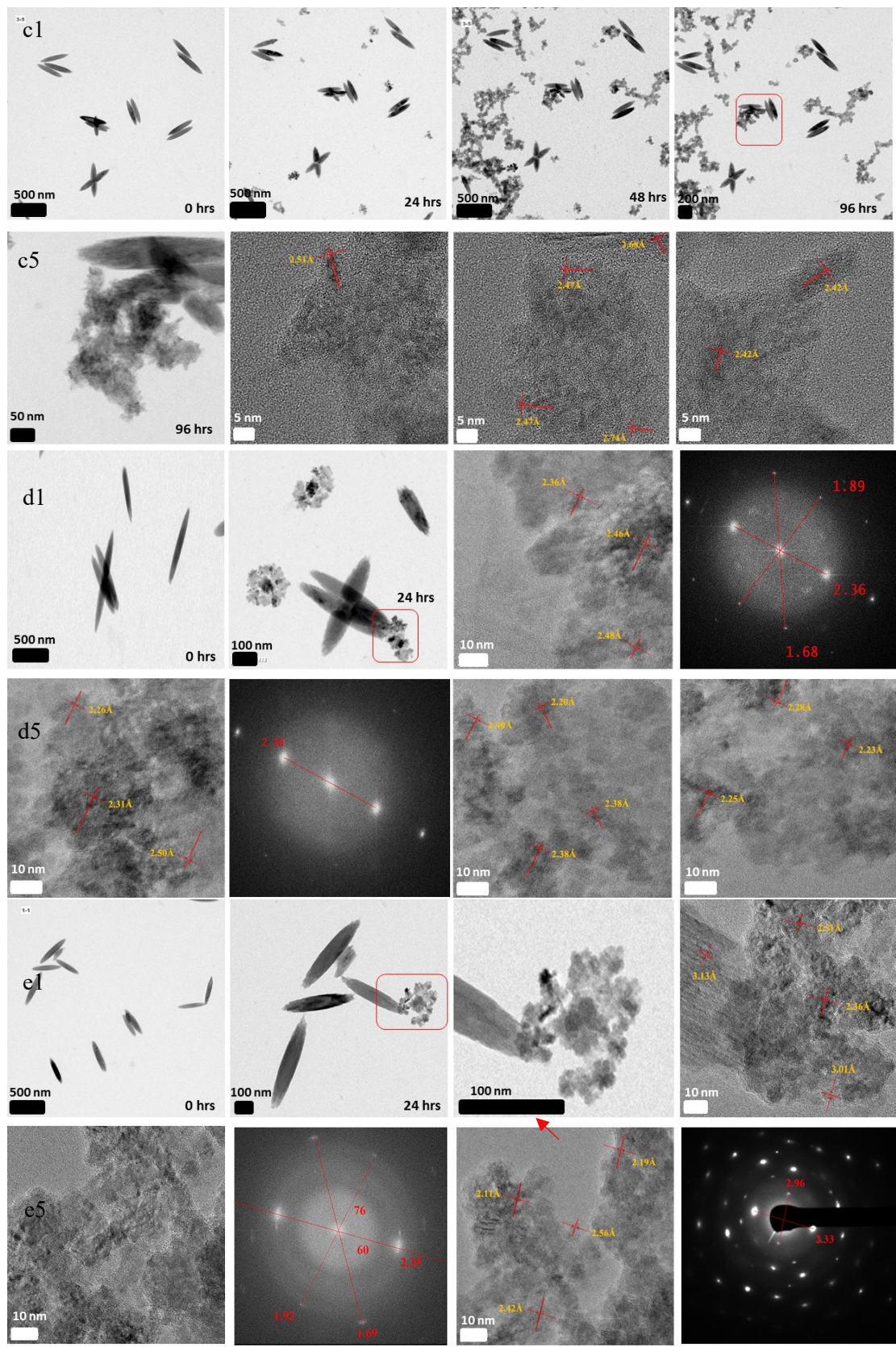


Figure S8. TEM of LP particles upon reaction with 10mM Fe(II)_(aq) after 24hrs, 48hrs, 96 hrs, 120hrs, and 132hrs. The selected particles in the boxes show the breakage of the

LP into various pieces upon reaction. Identifiable lattice fringes of the broken fragments with spacings at 4.97\AA for the (020) plane of GT and 2.49\AA for the (130) plane of LP were observed.





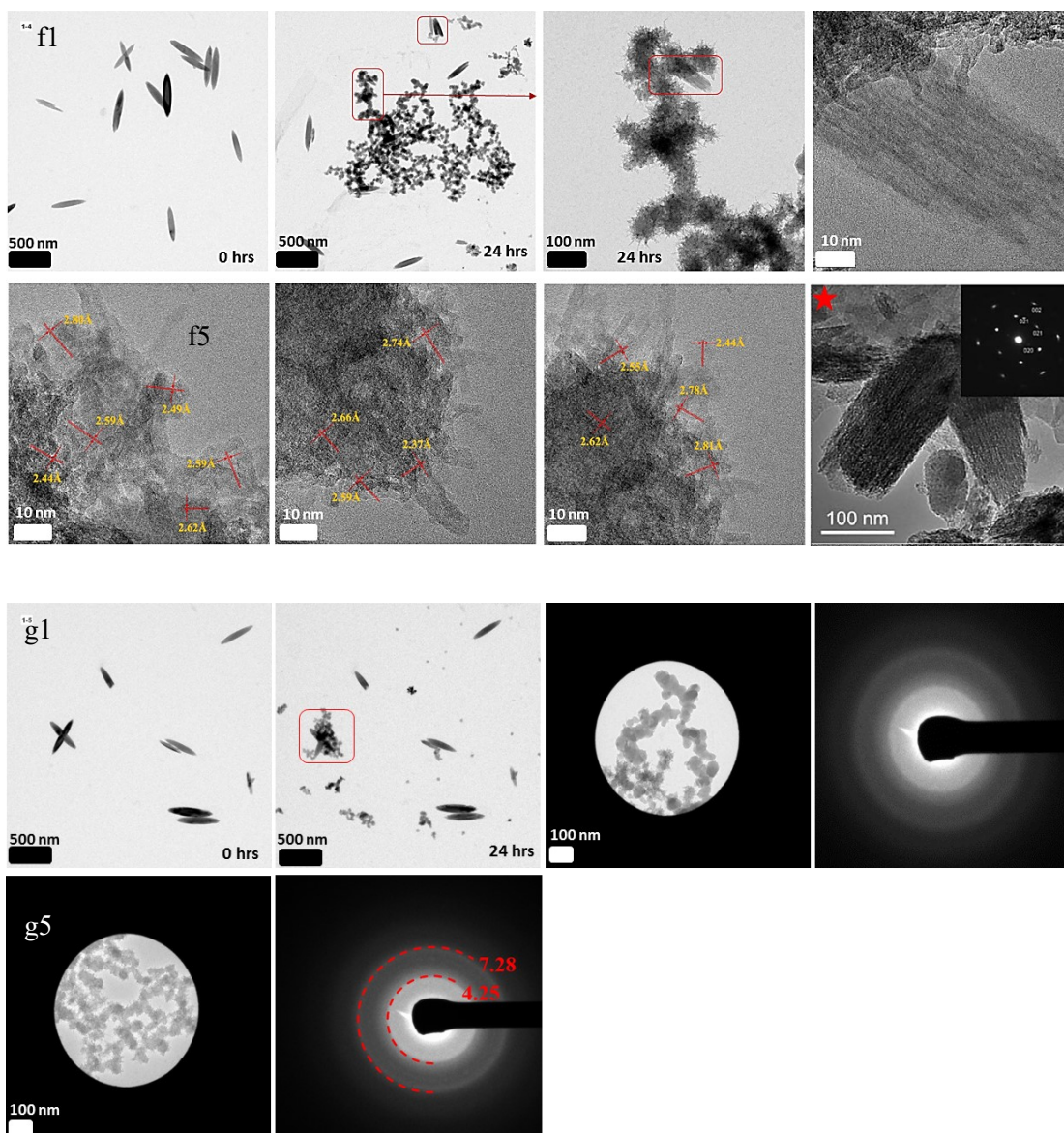
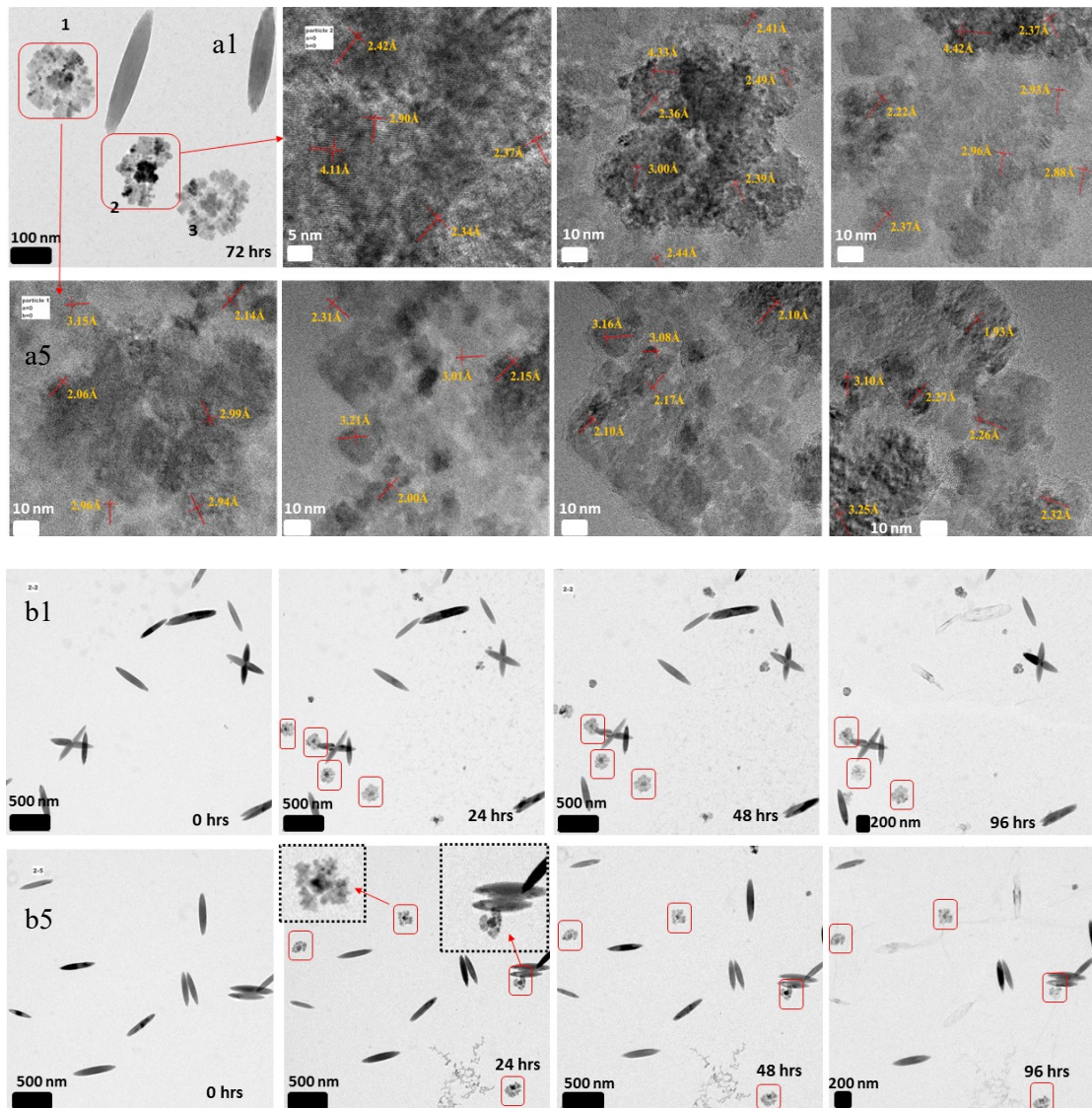


Figure S9. TEM and SAED of LP particles upon reaction with 10mM Fe(II)_(aq) after 24hrs, 48hrs, and 156hrs. The selected particles in the boxes show the breakage of the LP particle's ends to form nano-agglomerates, core-shells, and caterpillar-like particles. Identifiable lattice fringes with spacing's at 1.77Å-(221), 2.19Å-(140), 2.21Å-(210), 2.26Å-(121), 2.28Å-(200), 2.45Å-(111), 2.49Å-(040), 2.54Å-(101), 2.59Å-(021), 2.67Å-(130), 4.18Å-(110) of GT and 2.34Å-(020), 2.36Å-(111), 2.47Å-(130) of LP were observed. Diffraction rings and spots with spacing's at 2.09Å-(220), 2.30Å-(200) for GT and 1.18Å-(222), 1.49Å-(220), 1.62Å-(112), 2.36Å-(111) of LP were observed. It is noted that image f8 with a star on it was taken from Guo and Barnard⁸⁷ for better comparison on GT particles produced in nature from saprolite soils.



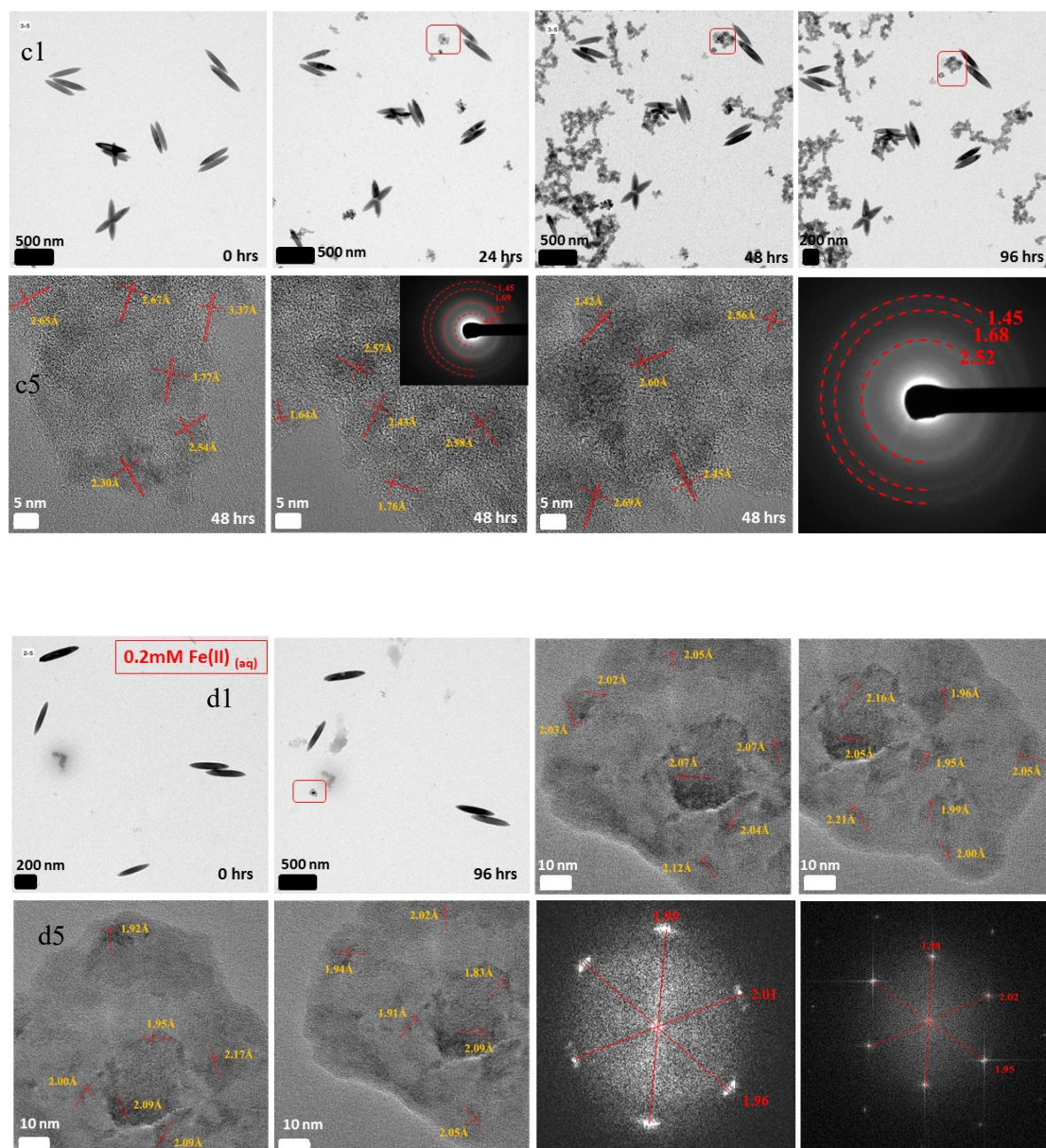


Figure S10. TEM and SAED of LP particles upon reaction with 10mM and 0.2mM $\text{Fe(II)}_{(\text{aq})}$ after 24hrs, 48hrs, 72hrs and 96hrs. Unless marked as 0.2mM $\text{Fe(II)}_{(\text{aq})}$, all images correspond to the 10mM $\text{Fe(II)}_{(\text{aq})}$ reactions. The selected particles in the boxes show the core-shell phase that forms upon the reaction of LP with $\text{Fe(II)}_{(\text{aq})}$. Identifiable lattice fringes with spacing's at 2.00Å-(131), 2.17Å-(140), 2.00Å-(131), 2.26Å-(121), 2.44Å-(111), 2.49Å-(040) for GT and 1.93Å-(002), 2.36Å-(111), 2.96Å-(110) of LP were detected. Diffraction rings and spots with spacing's at 1.45Å-(061), 1.68Å-(240), 2.01Å-(131), 2.52Å-(101), 4.17Å-(110) for GT and 1.95 Å-(150) of LP were observed.

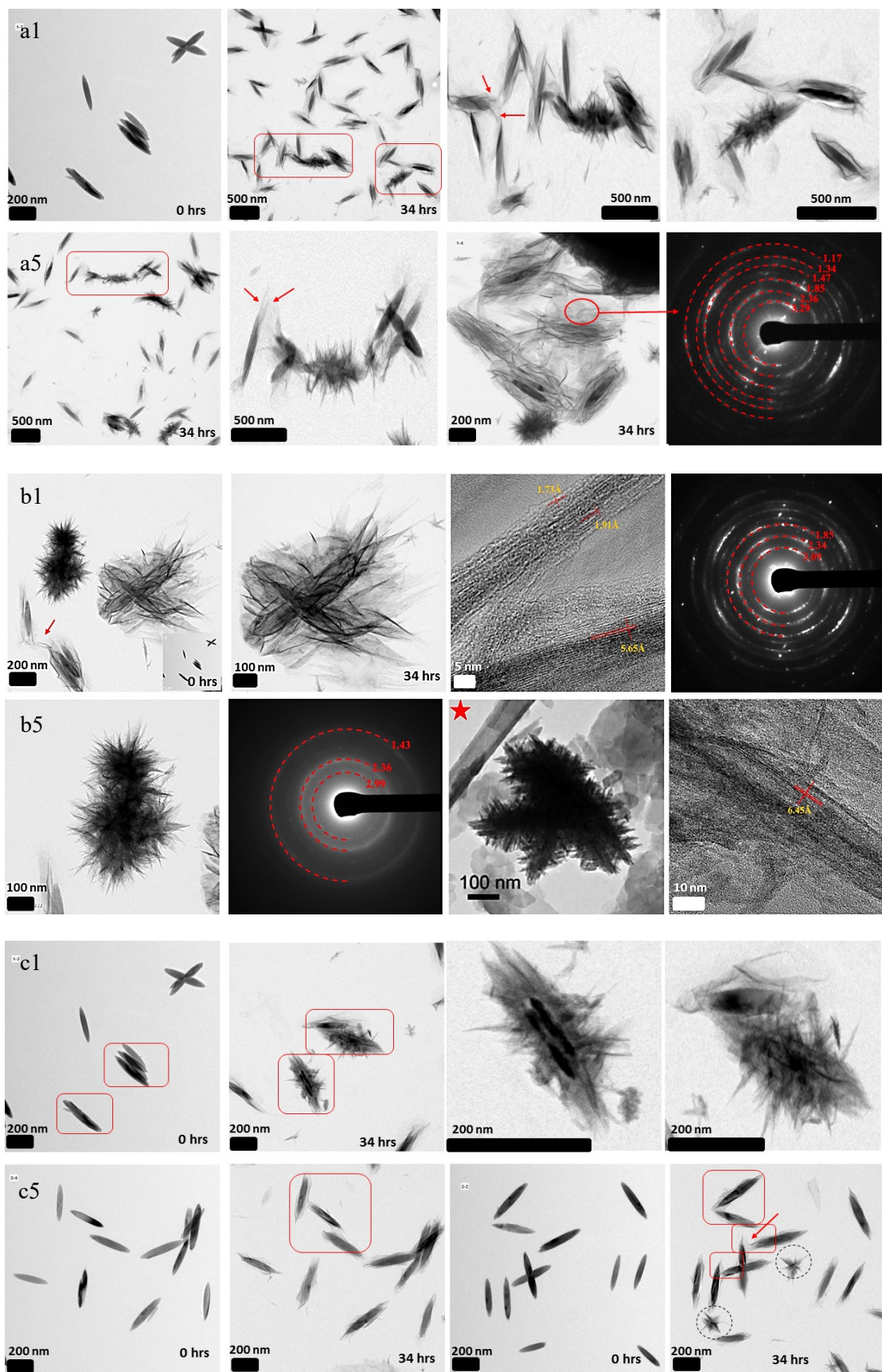
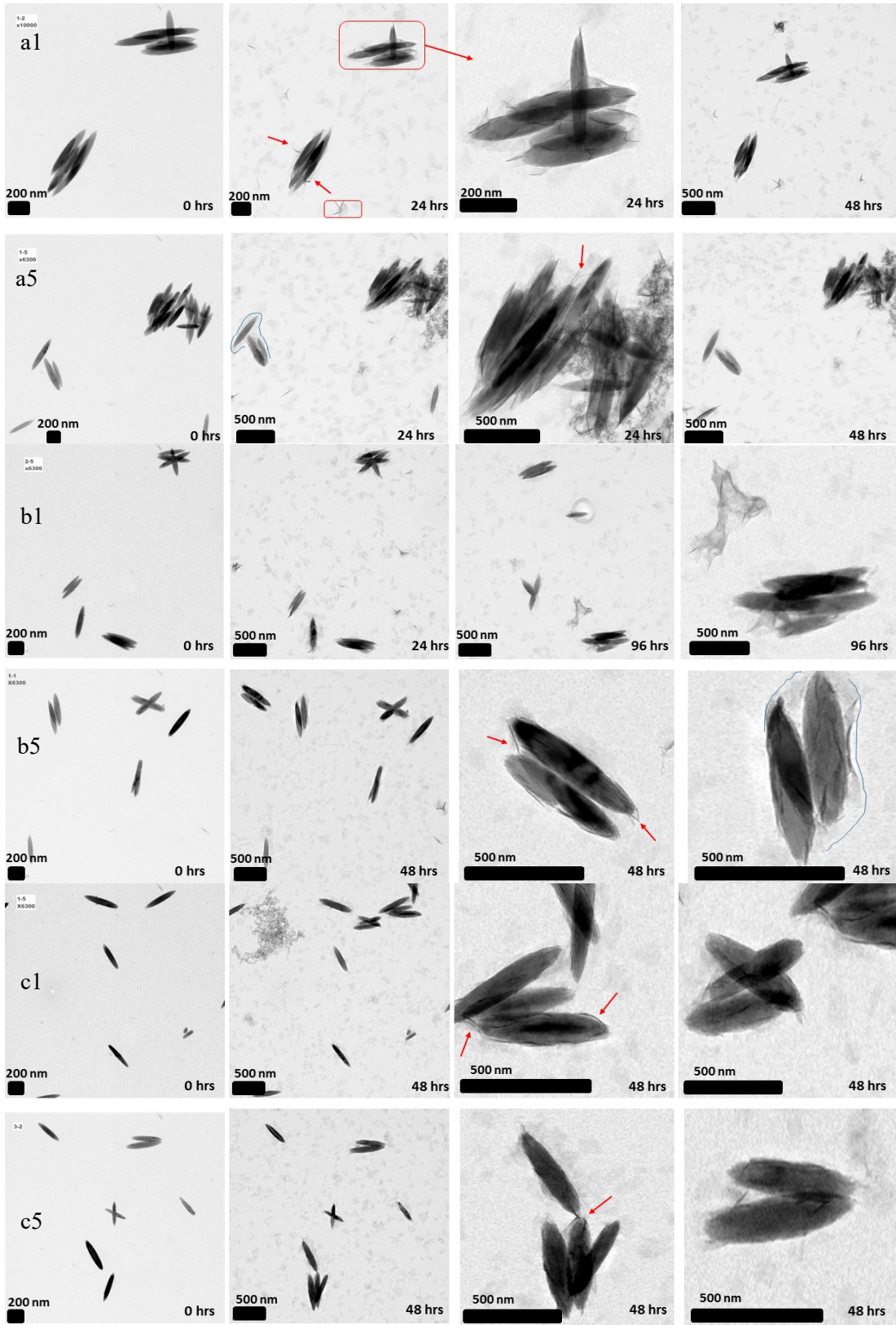


Figure S11. TEM and SAED of LP particles upon reaction with 10mM Fe(II)_(aq) after 34hrs. The selected particles in the boxes show the thin-film-like matrix around the

reacted LP particles and attachment through the thin-film-like matrix to form caterpillar-like particles. The arrows in the images highlight the nano-wire antennas (as shown in Figure 2) of reacted LP particles and their participation during attachment. Particles circled in a dashed line represent small star-shaped caterpillar-like particles. Diffraction rings with spacing's at 1.34\AA -(260), 1.47\AA -(241), 1.80\AA -(211), 2.30\AA -(200) for GT and 1.43\AA -(171), 1.85\AA -(022), 2.36\AA -(111), 2.99\AA -(110), 3.29\AA -(021) of LP were observed. It is noted that image b7 with a star on it was taken from Guo and Barnard⁸⁷ for a better comparison of GT Christmas tree particles produced in nature from saprolite soils.



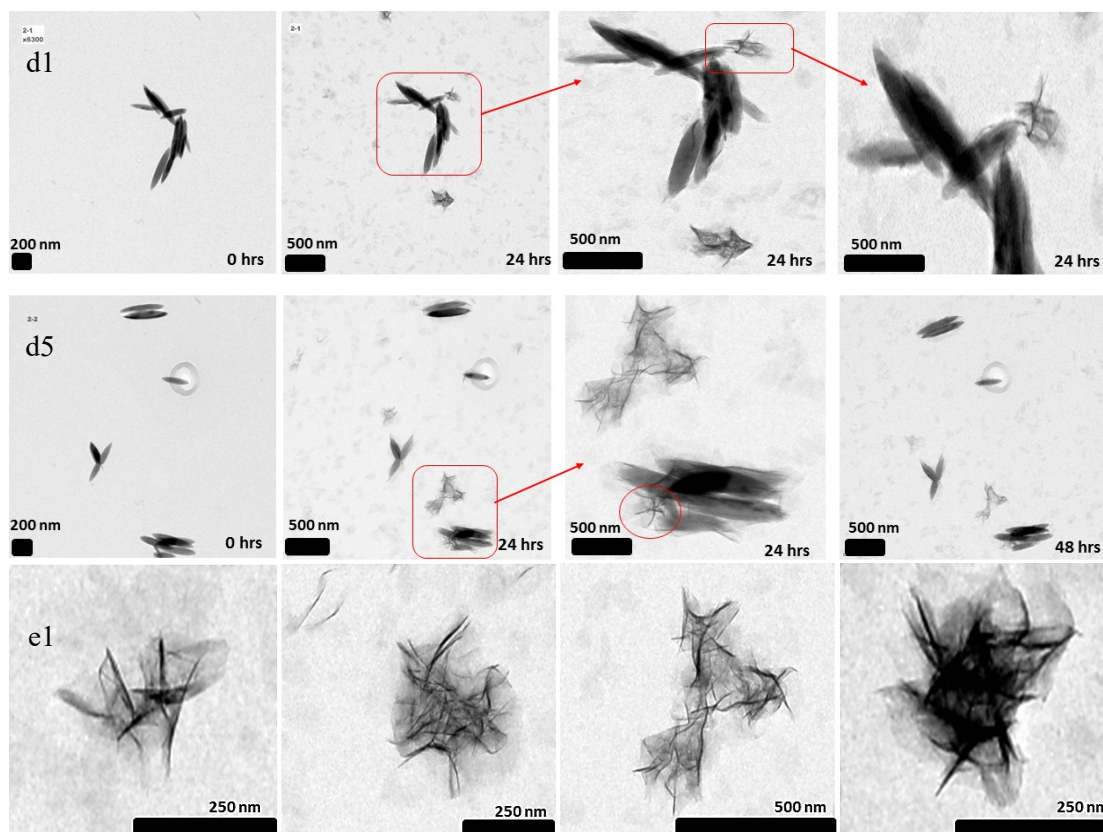


Figure S12. TEM of LP particles upon reaction with 0.2mM Fe(II)_(aq) after 24hrs, 48hrs and 96hrs. The selected particles in the boxes show the thin-film-like matrix around the reacted LP particles, particle attachment through the thin-film-like matrix, and formation of star-like nano-wire agglomerates. The arrows displayed in the images along the particles highlight the nano-wire antennas and peeling of nano-wires of the reacted LP.